JOURNAL OF APPLIED ELECTROCHEMISTRY 22 (1992) 628–637

Secondary processes during tantalum electrodeposition in molten salts

L. P. POLYAKOVA, E. G. POLYAKOV, A. I. SOROKIN, P. T. STANGRIT

Institute of Chemistry, Kola Scientific Centre of the USSR Academy of Sciences, 184200 Apatity, CIS

Received 19 September 1988; revised 3 September 1991

A comparative study of cathodic and anodic processes during the electrolysis of tantalum containing chloride and chloride-fluoride melts is presented. The substitution of chloride ions by fluoride ions in the ligand shells of Ta(IV) and Ta(V) species is proposed as the basis for a mechanism for the formation of sludge and the outgrowth of films from the electrode over the surface of the electrolyte during tantalum electrodeposition employing a soluble anode configuration.

1. Introduction

The processes of electrowinning and refining of refractory metals from halide melts are known to be accompanied by the formation of sludge and films which grow out from the cathode along the electrolyte surface, sometimes covering the whole inter-electrode space [1–3]. The nature of these processes has been discussed previously [1, 2, 4–6]. On the basis of a comparative study of processes involved in the anodic dissolution of tantalum and the cathodic reduction of tantalum species in the ternary eutectic melt of sodium chloride, potassium chloride and caesium chloride (30 : 24.5 : 45.5 mol %) (m.p. 480° C) containing potassium heptafluorotantalate and sodium fluoride additives, evidence is reported from which the mechanism of the secondary reactions, associated with and complicating the electrode processes, can be suggested.

The electrode processes which occur during the electrolysis of tantalum containing melts have been discussed previously and found to depend upon anion and solute compositions. These data are collected in Table 1. Numerous interpretations of the data have arisen, in part due to the differences in composition and temperatures. Moreover, where melts of the same composition have been used, experimental data can vary between authors. For example, in the extensively employed LiCl–KCl solvent, the average mean valency of dissolved tantalum varies between 3.04 and 5.0. Only two studies report the passivation of the anode by $KTaCl_6$ [9, 16] and Suzuki [12] claims the stable fixation of the plateau on the cathodic chronopotentiograms is associated with reduction of Ta(IV) → Ta(II).

There are no accepted mechanistic pathways for the discharge of tantalum ions from chloride–fluoride melts. Early studies [21, 22] reporting insensitivity of the polarization curves to additions of Ta_2O_5 to the melts and the liberation of CO and CO_2 at the anode must be regarded with caution. The pathway proposed by Rameau [23] is not acceptable in view of the critique in [31]. Following the development and investigations of the Union Carbide Fluoride process, the accepted reduction pathway from Ta(V) species in fluoride melts involved the two steps:

$$Ta(V) \longleftrightarrow Ta(II)\ (solid)$$

$$Ta(II)\ (solid) \longrightarrow Ta(O)$$

Taxil [30], in a recent paper, advocated that the pathway is a one step process. A one step process has also been proposed for the reduction of Ta(V) species from fluoride solutions containing tantalum oxyfluoride species [24, 31].

In this paper an attempt is made to clarify these contradictions, especially in reference to the chloride–fluoride and fluoride electrolytes as well as to explain, with the aid of the concept of discrete discharge of complexes, the formation of sludge and films covering the electrolyte surface in mixed ligand electrolytes [33].

2. Experimental details

The salts used in this work were KCl, CsCl and NaF of 'special superpure' grade, NaCl of 'chemical pure' grade and K_2TaF_7 of 'high purity' grade. In spite of the nominally high purity, organic impurities are often present which undergo pyrolysis at elevated temperatures in inert atmospheres and lead to dispersed carbon in the melts which can distort the shape of the voltammograms. Calcination of the salts, followed by aqueous dissolution, filtration and recrystallization enabled these impurities to be removed. Final drying of the salts was achieved at reduced pressure.

The eutectic salt mixture was heated stepwise under a vacuum to 400° C. The cell was then filled with argon and the temperature adjusted to its final value. Commercial K_2TaF_7 was recrystallized from hydrofluoric acid, washed with ethanol and dried in vacuum at 110–120° C. X-ray and i.r. spectroscopy was used to establish that the product was free of significant amounts of oxide impurities. (It will be shown later that oxide impurity is influenced more by the composition of the melts). Purification of the inert, head

0021-891X/92

Table 1. Summary of the electrochemistry of tantalum

Melt	*Solute and/or mean valency*	*Temperature/°C*	*Reduction pathway*	*Notes*	*Ref.*
LiCl–KCl	A.d. n_{ave} = 3.04–5.0	400		$j_a \leqslant 0.2\,A\,cm^{-2}$ – Ta(III), Ta(II) $j_a > 0.7\,A\,cm^{-2}$ – Ta(V) 3Ta(II) → Ta^0 + 2Ta(III)	[7]
NaCl–KCl	A.d. n_{ave} = 3.2–4.0	700		n_{eq} = 4	[8]
LiCl–KCl	A.d. n_{ave} = 3.7–5.0	360–600		Passivation of the anode by $KTaCl_6$	[9]
NaCl–KCl	A.d. n_{ave} = 2.76–2.98	700–900		Ta^0 is in equilibrium with Ta(II) and Ta(III). Disproportionation	[10]
LiCl–KCl	A.d. n_{ave} = 4	500–675		n_{eq} = 4	[11]
LiCl–KCl	$TaCl_4$	500–675	Ta(IV) → Ta(II) Ta(II) → Ta(O)	The one-step oxidation Ta^0 → Ta(IV)	[12]
LiCl–KCl	A.d.	450	Ta(IV) → Ta(O)	Extra waves immediately after anodic dissolution	[13]
NaCl–KCl	A.d. Low j_a – n_a = 3.0–4.0 High j_a – n_a = 5	800		Ta(IV) + Ta = 2Ta(II) $\log k = -13/T + 0.54$	[14]
NaCl–KCl	Lower tantalum chlorides	750–850	Ta(IV) → Ta(II) Ta(II) → Ta(O)	After the addition of $TaCl_5$ Ta(V) → Ta(II), Ta(II) → Ta(O)	[15]
LiCl–KCl	A.d. Low j_a – Ta(IV) High j_a – Ta(V)	Up to 600		Passivation of the anode by $KTaCl_6$	[16]
CsCl–KCl	A.d. n_{ave} = 3.36–3.77	600–800		Red-purple colour of the melt. Disproportionation	[17]
CsCl	A.d. n_{ave} = 3.87–4.20	700		Codeposition of Ta^0 and lower valency compounds after displacement of CsCl by LiCl.	[18]
NaCl–KCl	$TaCl_5$	750–900		n_{eq} = 2.1–3.2	[19]
NaCl–KCl	A.d. n_{ave} = 2.2–4.6	780			[20]
NaCl–KCl	K_2TaF_7	850	Ta(V) → Ta(III) Ta(III) → Ta(O)	Anodic gases: CO, CO_2	[21]
NaCl–KCl + 10 wt % NaF	A.d. n_{ave} = 4.3–5.0	700		Depolarization after NaF addition	[8]
NaCl–KCl	K_2TaF_7	750	Ta(V) → Ta(III) Ta(III) → Ta(O)	Anodic gases: Co, CO_2	[22]
KCl	K_2TaF_7	930	Ta(V) → Ta(III) Ta(III) → Ta(O)	The preceeding reaction 3Ta(V) + 2Ta → 5Ta(III)	[23]
KCl–KF	K_2TaF_7	700	Ta(V) → Ta(O)		[24]
LiCl–KCl + 5 wt % LiF	A.d. n_{ave} = 3.75–4.69	400		Depolarization after LiF addition	[7]
NaCl–KCl + 1 wt % $TaCl_5$ + 2 wt % NaF	A.d. n_{ave} = 4.42–4.95	800		Depolarization after NaF addition	[19]
LiCl–KCl + KF	$TaCl_5$	400–550	Ta(V) → Ta(O)	Until F-ion addition Ta(V) → Ta(III) Ta(III) → Ta(O)	[25]
LiF–NaF–KF	K_2TaF_7	640–680	Ta(V) → $Ta(II)_s$ $Ta(II)_s$ → Ta(O)	Alumina salt bridge (contaminator)	[26]
NaF–KF	K_2TaF_7	730	Ta(V) → $Ta(II)_s$ $Ta(II)_s$ → Ta(O)		[27]
LiF–NaF	K_2TaF_7	800	Ta(V) → $Ta(II)_s$ $Ta(II)_s$ → Ta(O)		[28]

Table 1 (Continued)

Melt	*Solute and/or mean valency*	*Temperature/°C*	*Reduction pathway*	*Notes*	*Ref.*
LiF–NaF	K_2TaF_7	850–1050	Ta(V) → $Ta(II)_s$ $Ta(II)_s$ → Ta(O)	Ni working electrode-3 waves; Mo working electrode-1 wave	[29]
LiF–NaF–KF	K_2TaF_7	550–1050	Ta(V) → Ta(O)		[30]
LiF–NaF Na_3AlF_6	Ta_2O_5 or $NaTaO_3$	1000	Ta(V) → Ta(O)		[31]
KCl–KF	K_2TaF_7 and Ta_2O_5	700	Ta(V) → Ta(O)	Discrete discharge of fluoride and oxygen	[24]

A.d. Anodic dissolution.
n_{ave} Average valency.
n_{eq} Equilibrium valency.

space, gas is important [34] in these studies and a commercial apparatus "PG" was used. Sequentially, the argon was dried and purified by passing through active alumina, nickel–chromium catalyst and synthetic zeolites. The water content was reduced to 10^{-4} mg m^{-3} and the oxygen content was 10^{-5} to 10^{-6} vol%.

The cell used in the work is illustrated in Fig. 1. Selection of the materials for the cell body and crucible for the electrolyte was made in the light of the following factors. It is known that gaseous $TaCl_5$ at the temperatures employed in the electrochemical investigations (500–800° C) reacts with quartz [35, 36]:

$$2TaCl_5 + SiO_2 \longrightarrow 2TaOCl_3 + SiCl_4 \qquad (1)$$

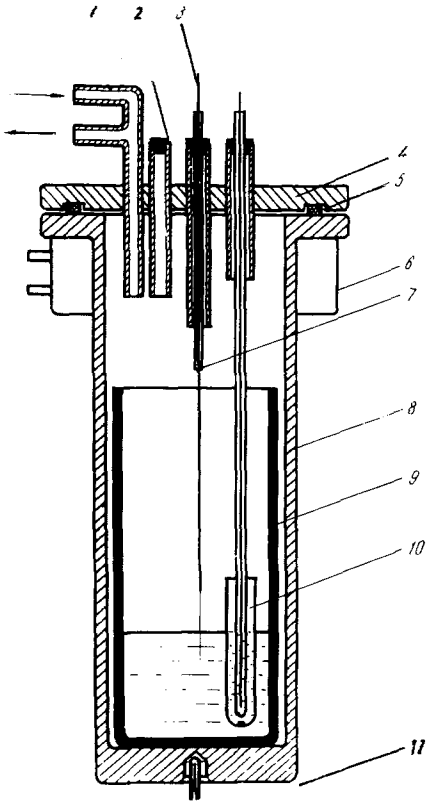

Fig. 1. Experimental cell. (1) Gas inlet/outlet tube, (2) addition tube, (3) working electrode, (4) stainless steel head, (5) 'O'-ring, rubber or Teflon, (6) water cooling jacket, (7) alumina support tube, (8) stainless steel can, (9) glassy carbon crucible, (10) reference electrode and (11) thermocouple.

The same reaction with tantalum pentachloride dissolved in the melt can not be ruled out moreover, if there are significant amounts of Li^+ or even Na^+ in the melt, $TaCl_5$ may be lost [2, 8, 17] thus:

$$TaCl_6^-(soln) \longrightarrow TaCl_5(g) + Cl^- \qquad (2)$$

The reaction of quartz with lower valent chlorotantalum species has also been pointed out [37]. Since Pyrex glass contains silica, similar reactivity with this material is to be expected. Indeed, Bailey [13] suggested that some peaks in their observed voltammograms might have resulted from products of the reaction between the glass sleeve of the working electrode and the tantalum species in the melt. Secondary reactions among cell materials and refractory metal chlorides leading to the formation (by disproportionation) of metallic films and low solubility oxychlorides have been described [38].

Although in his review [34], White claimed that it is possible to work for short times with alumina in contact with fluorides, it is necessary to note that even minimal amounts of oxide corrosion in melts containing complex fluorides of the refractory metals can lead to the formation of oxyfluoride complexes in the melt with characteristic voltammetric responses [39].

This problem arose in the classical work of Senderoff *et al.* [26] where an alumina salt bridge was used with the reference electrode. Their chronopotentiograms taken for the tantalum containing melts, reproduced in Fig. 2, contained three transition times at −1.0, −1.2 and −1.5 V, not associated with the solvent. The last of these was eliminated when the alumina was replaced by a boron nitride salt bridge [26]. The first two steps at −1.0 and −1.2 V were explained by a two step reduction pathway which involved the intermediate formation of TaF_2(s). By analogy with the previous results [39, 40], the interactions in the fluoride melts employed by Senderoff in a simplified way can be written as

$$4MF + M_2TaF_7(soln.) + Al_2O_3 \longrightarrow M_2TaOF_5 + 2M_2AlOF_3 \qquad (3)$$

$$2MF + M_2TaF_7(soln.) + Al_2O_3 \longrightarrow M_2TaOF_5 + 2MAlOF_2 \qquad (4)$$

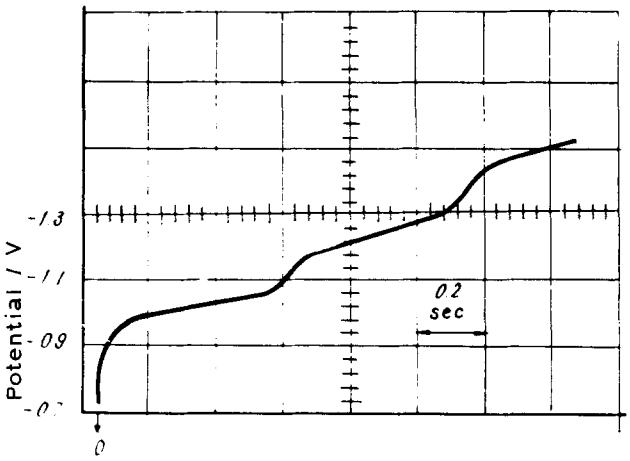

Fig. 2. Cathodic chronopotentiogram for K_2TaF_7 dissolved in KF–LiF–NaF, eutectic mixture (Flinak); concentration = 8×10^{-5} mol cm^{-3}; current density = 0.113 A cm^{-2}; temp. = 750° C; cathode, platinum [26].

$$4MF + M_3TaF_8(soln.) + Al_2O_3 \longrightarrow M_3TaOF_6 + 2M_2AlOF_3 \quad (5)$$

were M = Li, (Na, K). The replacement of Al_2O_3 by BN did not lead to the elimination of oxyfluoride complexes, since sintered BN contains 5 to 8 wt % of B_2O_3.

Earlier investigations of the interaction between KCl–KF–K_2TaF_7 electrolyte and Ta_2O_5 showed [24] that the characteristics of the voltammograms changed with the additions of Ta_2O_5 to the electrolyte, see Fig. 3. These data were interpreted to mean that oxyfluoride complexes were formed in addition to fluoride complexes of tantalum which were discharged at −1.4 and −1.2 V, respectively, against the Ag/AgCl reference electrode. Thus the exact coincidence of the potential differences of the first and second peaks in these voltammograms and those of Senderoff's chronopotentiometric data, together with the change in the relative heights of the first and second peaks with K_2TaF_7/Ta_2O_5 ratio (in general terms the TaF_7^{-2}/O^{-2}) leads to the conclusion that contact between alumina and these K_2TaF_7 containing melts has serious consequences. These ideas explain some of the difficulties Senderoff *et al.* had in interpreting the τ_2/τ_1 ratio which differed significantly from experiment to experiment, perhaps due to the duration and degree of contamination by oxide ions. Further τ_2 would be variable since it is related to the concentration of oxyfluoride complex. The two step mechanism has been further criticized [2] because of the inability to identify the intermediate. Nevertheless, in spite of these difficulties, Senderoff's mechanism has persisted in the tantalum literature.

Consequently, the stringent requirements for container materials reduce the choice from among the noble metals, and glassy carbon crucibles and ampules. Glassy carbon ware is particularly suitable since it has low liquid and gas permeability (10^{-8}–10^{-12} cm^2 s^{-1} for He), good mechanical strength (σ_c = 350–400 MPa, σ_β = 160–170 MPa) hardness, low thermal conductivity (3–6 W m^{-1} K^{-1}) and low electrical resistance (40–50 × 10^{-4} Ω cm). It possesses extreme thermal stability and withstands thermal cycling with rates as high as 200 K s^{-1}. Its particular structure and the low open porosity (1–2%) impede the interdiffusion of impurity atoms through the glassy carbon/melt interphase helping to ensure reliable experimental data.

The selection of materials for the working electrode is also critical, especially at temperatures in excess of 500° C. Taxil [29] demonstrated the dramatic influence of material on the voltammetric responses for tantalum melts and Fig. 4 illustrates the differences in response for Mo and Ni working electrodes. Recently others [41] have reported voltammograms distorted by

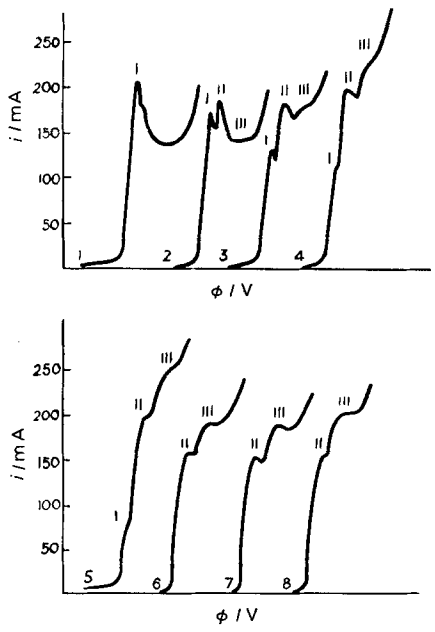

Fig. 3. Linear sweep voltammograms in KCl–KF–K_2TaF_7 and KCl–KF–K_2TaF_7–Ta_2O_5 melts at various Ta_2O_5/K_2TaF_7 ratios; V = 4 V min^{-1}. Curves are shifted along the potential axis. Ta_2O_5/K_2TaF_7 ratios: (1) 0, (2) 0.0377, (3) 0.097, (4) 0.179, (5) 0.270, (6) 0.372, (7) 0.480 and (8) 0.667 (K_2TaF_7 initial content: 9.2 wt %, curve 1). Reduction waves: (I) $[TaF_8]^{3-}$, (II) $[TaOF_6]^{3-}$ and (III) $[TaO_2F_4]^{3-}$.

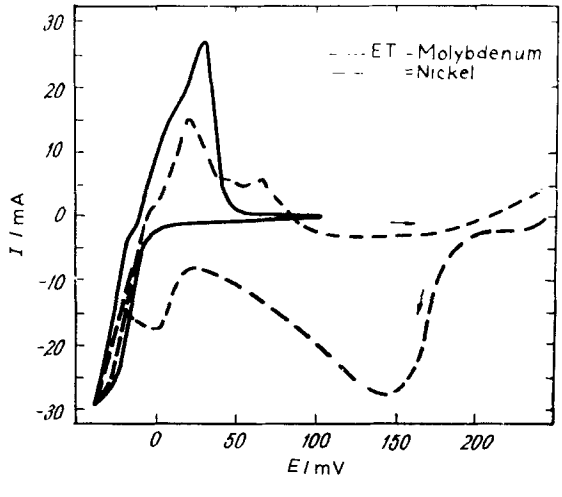

Fig. 4. Reduction of TaF_7^{2-} ions at 1050° C: the formation of intermetallic compounds at the nickel working electrode [29].

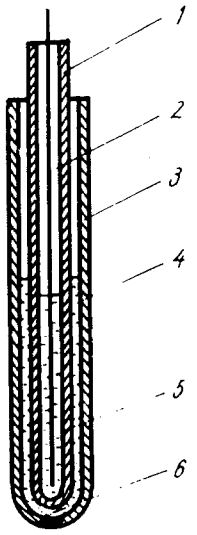

Fig. 5. Reference electrode design. (1) Alumina tube, (2) silver wire, (3) glassy carbon shell, (4) base electrolyte CsCl–KCl–NaCl, (5) base electrolyte + 2 wt % AgCl and (6) graphite plug.

the cathodic formation of intermetallic TiPt compounds. Extreme care should be taken not to assign the additional waves to stages in the discharge of the cations.

The selection of a reference electrode is traditionally complicated for chloride–fluoride melts. In the present experiments, a silver electrode: Ag/AgCl (2.0 wt %, NaCl–KCl–CsCl (eutectic) was employed. The construction of the electrode is illustrated in Fig. 5. It minimized the uncertainty of the electrode potential introduced by an alumina diaphragm and graphite plug/glassy carbon tube which protected the alumina from the aggressive fluoride melt [42, 43]. The graphite plug in the glassy carbon shell was rapidly impregnated (~ 0.5 h) with the electrolyte to provide a stable liquid junction.

The cell components were housed in a thick walled, hermetic, stainless steel container which minimized temperature gradients in the electrolyte. The temperature was maintained to within about $\pm 0.5°$ C by a VRT-3 regulator. The electrochemical studies employed PI–50–1 and P–5848 potentiostats and a PO–5122 oscillographic polarograph. Current efficiency measurements of the anodic dissolution process were performed with the aid of an IPT–1 integrator.

3. Results and discussion

3.1. *Solvent quality*

The quality of the base melt after preparation was established under the standard conditions recommended in the literature [34]. The voltammogram for the NaCl–KCl–CsCl base electrolyte shown in Fig. 6 demonstrates the absence of quantities of cationic and anionic impurities sufficient to distort the electrochemical measurements.

3.2. *Cathodic reduction of tantalum in chloride melts*

The question of disproportionation reactions of tantalum often arises in papers concerning the electrode processes in chloride melts [7, 10, 17]. The authors of [10] proposed that it is the Ta(IV) ions which undergo disproportionation whereas in [7] it is claimed to be the Ta(II) ions. Alternatively, a third group has suggested that the disproportionation is a characteristic of the lower oxidation state polynuclear species, although direct evidence was not obtained. The indirect evidence showed that $n = 4$, that the cathodic chronopotentiograms contained a stable single transition time, and the voltammetric cathodic and anodic cycles possess almost equal charges. These data imply the absence of long lived intermediates between Ta(IV) and Ta(O), although the formation of ions of valency less than 4 in the LiCl–KCl and NaCl–KCL melts cannot be ruled out since the presence of monovalent cations in the second coordination shell around the tantalum ions leads to an increase in the average valency of the tantalum species in the melt, thus decreasing the probability of forming lower valency species [17, 18]. The recent studies [44] of tantalum in the ternary NaCl–KCl–CsCl eutectic contribute to the elucidation of these problems and are reiterated here.

Figure 7 illustrates the voltammetric response of the base melt containing tantalum pentachloride where the ion present is probably the $TaCl_6^-$ species [45]. Potentiostatic electrolysis at potentials corresponding to the first wave does not produce a deposit on, or a change in, the electrode surface. Controlled potential electrolysis at potentials corresponding to the second wave resulted in a deposit, identified by X-ray diffraction as metallic tantalum. Consideration, according to

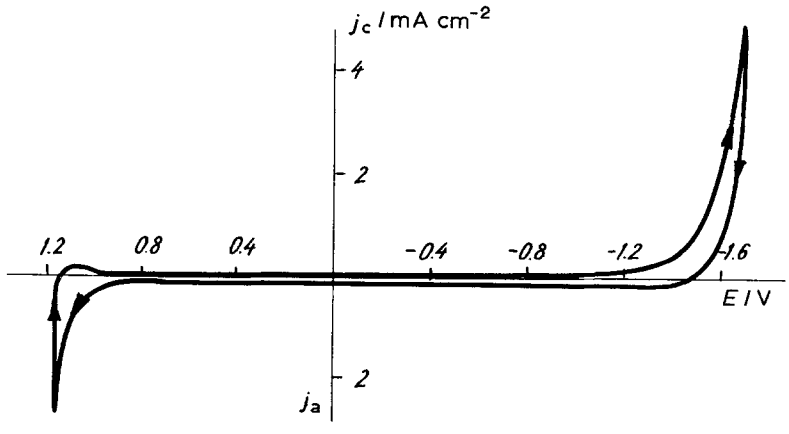

Fig. 6. Voltammogram for CsCl–KCl–NaCl. Glassy carbon working electrode; sweep rate 0.1 V s^{-1}; reference electrode is Ag/AgCl; temp. 620° C.

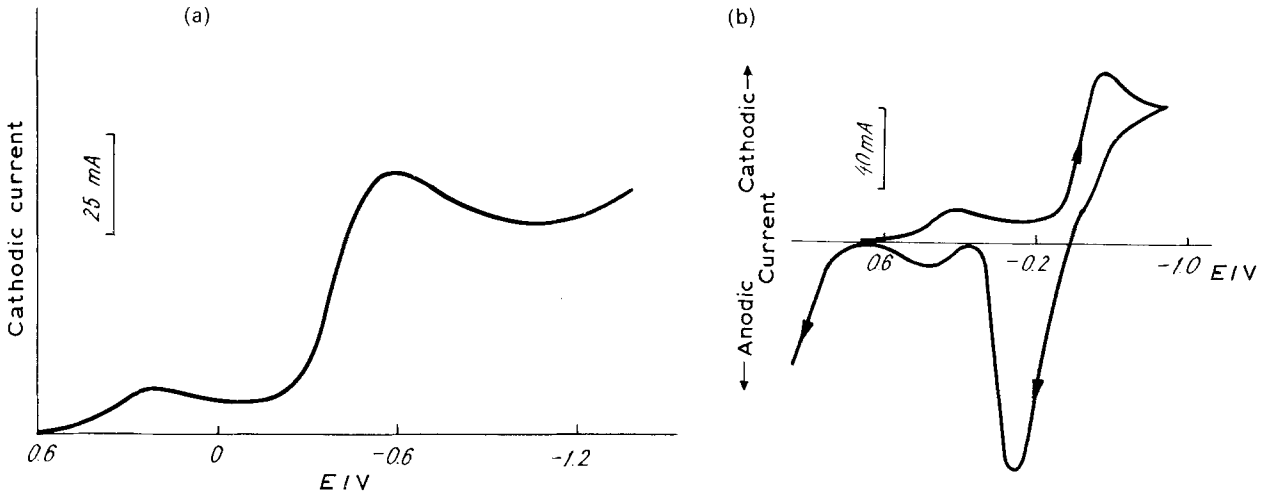

Fig. 7. Voltammograms for CsCl–KCl–NaCl–$TaCl_5$ melt. (a) Cathodic curve: $TaCl_5$ concentration = 2.51 wt %; electrode area = 0.14 cm^2; sweep rate = 1.33 $V s^{-1}$; temp. = 587° C. (b) Cyclic curve: $TaCl_5$ concentration = 1.90 wt %; electrode area = 0.26 cm^2; sweep rate = 1.33 $V s^{-1}$; temp. = 587° C.

diagnostic criteria [46], of the first and second stages of the cathodic voltammograms revealed that the first wave is a reversible one electron reduction of Ta(V) to Ta(IV), where the product of the reduction is soluble in the melt. Supporting evidence for this reaction was obtained from the voltammetric study of the reaction between such a melt containing Ta(V) ions and tantalum metal. The voltammograms revealed that the introduction of tantalum into the NaCl–KCl–CsCl–$TaCl_5$ melt resulted in the disappearance of the first cathodic wave and only the oxidative component corresponding to the Ta(V)/Ta(VI) couple was detected. This result indicates that the reaction:

$$4CsTaCl_6 + Ta + 6CsCl \longleftrightarrow 5Cs_2TaCl_6 \quad (6)$$

is shifted completely to the right. Examination of the electrolyte showed it was red purple in colour, as reported in [17] and that the crystals are optically isotropic and purple in transmitted light, characteristic of Cs_2TaCl_6 [47]. X-ray diffraction analysis confirmed the formation of this compound. Table 2 collates the weight loss data for the Ta specimens and the stoichiometry of Reaction 6. The investigation of the second reduction stage was carried out on the initial solution or in solutions where the Ta(V) was reduced to Ta(IV) by reaction with metallic tantalum. The results from the two studies are consistent. The voltammetric data indicate that the reduction of Ta(IV) to metal in the temperature region 500–700° C is irreversible [48].

Table 2. Tantalum corrosion data

Tantalum concentration/wt %		*Weight loss*/g	*Theoretical weight loss according to Reaction 6*/g
Before exposure	*after exposure*		
0	0.01	0.002	–
0.51	0.64	0.076	0.078
0.95	1.19	0.142	0.144
2.16	2.69	0.324	0.318

Weight of melt: 60 g; temp.: 650° C

3.3. *Cathodic reduction of tantalum species in chloride fluoride melts*

Several authors have reported the polarization of tantalum electrode processes in chloride melts when fluoride ions are added [2, 7, 8, 16, 19]. This phenomenon has been discussed in terms of the displacement of chloride ions from the ligand shell of the higher oxidation state tantalum ions by the fluoride ions [2], whereas Stangrit *et al.* [25] pointed to a change in mechanism for the reduction in the presence of fluoride ions. The voltammograms at the end of the substitution reaction with fluoride ion, in the temperature range 550–780° C, show the one step reduction of Ta(V) ions similar to that in the chloride–fluoride melt, NaCl–KCl–CsCl–K_2TaF_7 illustrated in Fig. 8. Using controlled potential electrolysis at potentials corresponding to the limiting current region

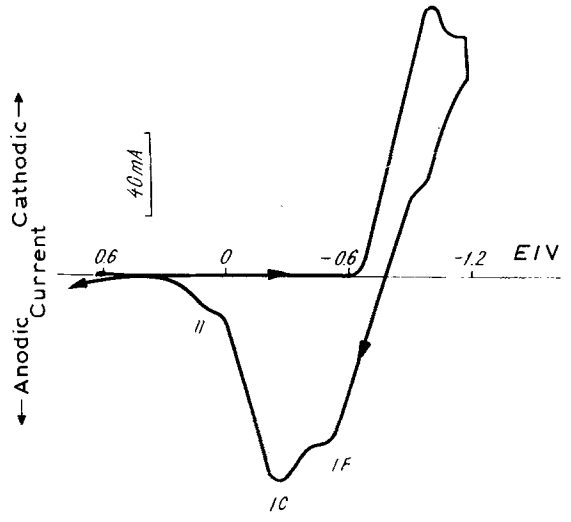

Fig. 8. Voltammogram for CsCl–KCl–NaCl–K_2TaF_7 melt. K_2TaF_7 concentration = 1.96 wt %; electrode area = 0.43 cm^2; sweep rate = 0.2 $V s^{-1}$; temp. = 680° C.

Table 3. Tantalum corrosion data

Temperature/°C	*Rate of corrosion*/g m^{-2} h^{-1}			
	CsCl–KCl–NaCl eut.	*Eut. + 5 wt % K_2TaF_7*	*Eut. + 10 wt % K_2TaF_7*	*Eut. + 10 wt % K_2TaF_7 + 5 wt % NaF*
680	2.1	7.1	7.4	22.0
720	2.7	19.7	16.2	30.5
760	4.1	21.0	20.3	32.7
800	4.5	25.1	24.3	34.3

of the wave, it was shown by X-ray analysis that tantalum metal was the product of the reaction. The absence of a conproportionation reaction to produce small amounts of lower valent ions occurring in chloride melts [2, 17] was confirmed in this paper by the corrosion data for tantalum in these melts (Table 3) and by the shape of the voltammograms. Analysis of the voltammograms reveals that the process of Ta(V) discharge to metal is irreversible [49].

The experimental evidence for Ta(V) reduction in mixed fluoride–chloride melts and of the Ta(IV) reduction in chloride melts shows that long lived intermediates are absent in the cathodic processes. Nevertheless, the electrowinning of tantalum from this electrolyte, in the presence of a tantalum anode, is accompanied by the outgrowth of films from the electrode over the electrolyte surface due to disproportionation of low valency compounds [1]. Thus, a study of the cathode processes alone does not provide a satisfactory basis for an explanation of the mechanism of these ancillary processes. These problems may be related to the products formed during the dissolution of the tantalum anode.

3.4. *Anodic dissolution of tantalum*

The anodic dissolution of tantalum was studied under conditions similar to those used in the cathodic studies. Tantalum plates (99.9 wt % pure) were used as anodes. Linear voltammetric data, as well as gravimetric data, were obtained. In the latter, identical amounts of charge were passed at different current densities. The current yields and the average valencies of dissolved tantalum for the three electrolytes studied are presented in Table 4.

Three regions can be recognized in the anodic volt-

Table 4. Dependencies of current yield (C_E) and average cation valency (n) on temperature, anodic current density (j_a) and electrolyte composition for anodic dissolution of tantalum

j_a /A cm^{-2}	*680° C*		*720° C*		*760° C*	
	C_E /g A^{-1} h^{-1}	n	C_E /g A^{-1} h^{-1}	n	C_E /g A^{-1} h^{-1}	n
CsCl–NaCl–KCl						
0.005	1.72	3.93	1.70	3.97	1.71	3.95
0.01	1.67	4.04	1.68	4.02	1.70	3.97
0.02	1.68	4.01	1.72	3.92	1.67	4.04
0.05	1.61	4.20	1.59	4.25	1.65	4.10
0.1	1.21	5.55	1.55	4.37	1.60	4.23
0.2	1.14	5.90	1.53	4.42	1.51	4.49
0.3			0.85	7.99	1.49	4.52
0.4					1.26	5.37
CsCl–NaCl–KCl: 10 wt % K_2TaF_7						
0.01	1.35	5.00	1.35	4.98	1.35	4.99
0.02	1.36	4.97	1.35	4.98	1.37	4.94
0.05	1.34	5.03	1.35	4.99	1.35	5.01
0.1	1.44	4.68	1.44	4.68	1.38	4.88
0.2	1.38	4.88	1.50	4.49	1.49	4.54
0.3	1.33	5.08	1.49	4.73	1.42	4.77
0.4	1.09	6.15	1.14	5.90	1.41	4.79
0.5					0.98	6.93
CsCl–NaCl–KCl: 10 wt % k_2TaF_7; 5 wt % NaF						
0.01	1.32	5.10	1.33	5.09	1.36	4.95
0.02	1.38	4.91	1.34	5.05	1.37	4.94
0.05	1.34	5.05	1.37	4.95	1.37	4.95
0.1	1.34	5.03	1.32	5.10	1.35	5.00
0.2	1.36	4.95	1.33	5.07	1.36	4.95
0.3	1.34	5.05	1.37	4.93	1.34	5.03
0.5	1.36	4.97	1.35	5.02	1.37	4.93
0.7	1.24	5.45	1.33	5.09	1.35	5.02

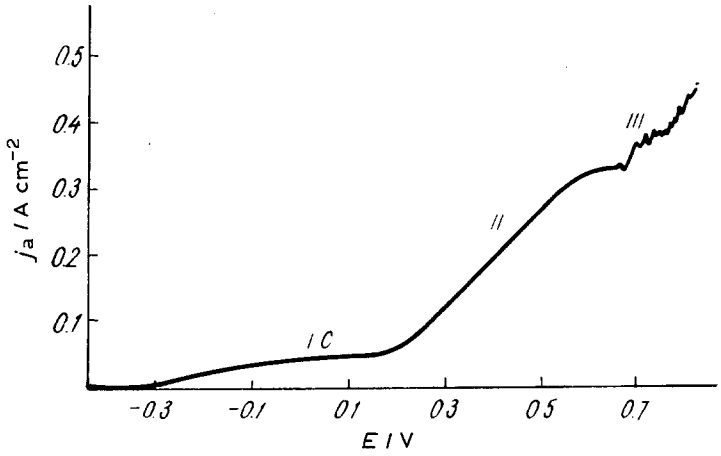

Fig. 9. Voltammogram of anodic dissolution of the tantalum anode in the CsCl–KCl–NaCl melt; temp. = 760° C; sweep rate = 0.2 V min^{-1}.

ammograms, Fig. 9 for a tantalum electrode in the NaCl–KCl–CsCl melt. In accordance with the data given in Table 4, the first region corresponds to the dissolution of tantalum to form Ta(IV) ions. The second region involves the oxidation of the Ta(IV) to Ta(V) ions and the third region involves the solvent anion oxidation to chlorine. The latter explains the sharp drop in current efficiency and the increased average valency values. The effect of increased temperature was to increase the current densities in the three regions.

The anodic dissolution of tantalum in the NaCl–KCl–CsCl–K_2TaF_7 melt proceeded in a more complex manner. A new wave, Fig. 10 region (IF), appears at more negative potentials, increases with increasing K_2TaF_7 concentration, and corresponds to an average valency of 5, Table 4. The shape of the curve resembles that in Fig. 9, i.e. there is a decrease in the average valency down to about 4.6 (region IC) when new regions (II) and (III) appear. The drop in current efficiency in (III) corresponds to chloride evolution. Similar behaviour was reported previously [19]. The region IF, which distinguishes Fig. 9 from Fig. 10, is associated with the dissolution of tantalum in the form of Ta(V) fluoride complexes. The small amount of free fluoride ions which determine the limiting current is

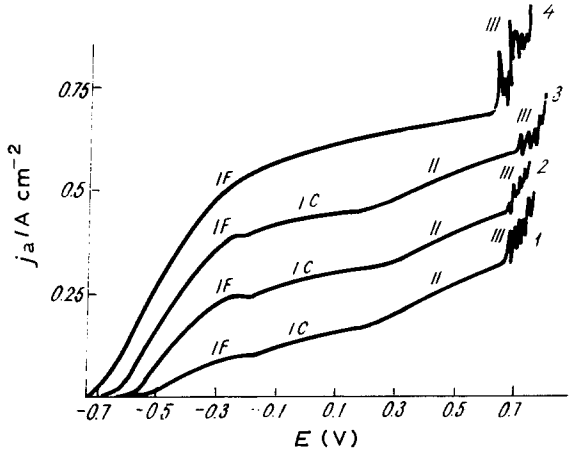

Fig. 10. Voltammetric curves for dissolution of the tantalum anode in the CsCl–KCl–NaCl–10 wt % K_2TaF_7 melt at 720° C against NaF concentration (wt %): (1) 0, (2) 1.49, (3) 2.91, and (4) 5.70. Sweep rate = 0.2 V min^{-1}.

formed by the dissociation of the TaF_7^{2-} or the partial substitution of fluoride ions by chloride ions in the ligand shell of Ta(V):

$$TaF_7^{2-} \longleftrightarrow TaF_6^{-} + F^{-} \quad (7)$$

or

$$TaF_7^{2-} + Cl^{-} \longleftrightarrow TaF_6Cl^{2-} + F^{-} \quad (8)$$

Other evidence in favour of the nature of the anodic wave (IF) is that it also appears when the K_2TaF_7 is replaced by NaF. The fact that the anodic dissolution of tantalum, to give fluoride or chloride complexes, proceeds at different potentials, can be accounted for by the decrease in the energy barrier due to the coordination of electrogenerated cations in the melts with fluoride as compared to chloride ions. Only $^{298}H_f^0$ data are available for these systems, and the enthalpy data show that the $^{298}H_f^0$ for TaF_5 is -437 ± 3 kcal mol^{-1} compared to $^{298}H_f^0$ for $TaCl_5$ of -182.25 ± 0.44 kcal mol^{-1} [50]. It is likely that this significant difference determines the observed discrete character of complexation.

The introduction of NaF in excess of the K_2TaF_7 increases the limiting current for the wave IF at the cost of the second (IC) and third (II) waves which correspond to the formation of Ta(IV) and Ta(V) chloro-complexes. The average valency of the dissolving tantalum is about 5 when the melt contains 5 wt % sodium fluoride.

The processes of anodic dissolution and cathodic reduction in NaCl–KCl–CsCl–K_2TaF_7 can be represented by the scheme outlined in Fig. 11. Depending upon the current density, the anodic dissolution may lead to chloride complexes of tantalum designated as $Ta(V)_{(Cl)}$ and $Ta(IV)_{(Cl)}$ oxidation states and fluoride complexes of $Ta(V)_{(F)}$. On the other hand only the fluoride complexes are discharged at the cathode since the starting electrolyte mixture contains K_2TaF_7. Thus the catholyte is excess free fluoride ions liberated by the discharge of the $[TaF_7]^{2-}$ complexes. The scheme shows two possible versions for the interaction between the free fluoride ions and the complex tantalum chloride ions formed during anodic dissolution. In the case of the contact with $Ta(V)_{(Cl)}$ ions only substitution of chloride by fluoride ions in the ligand

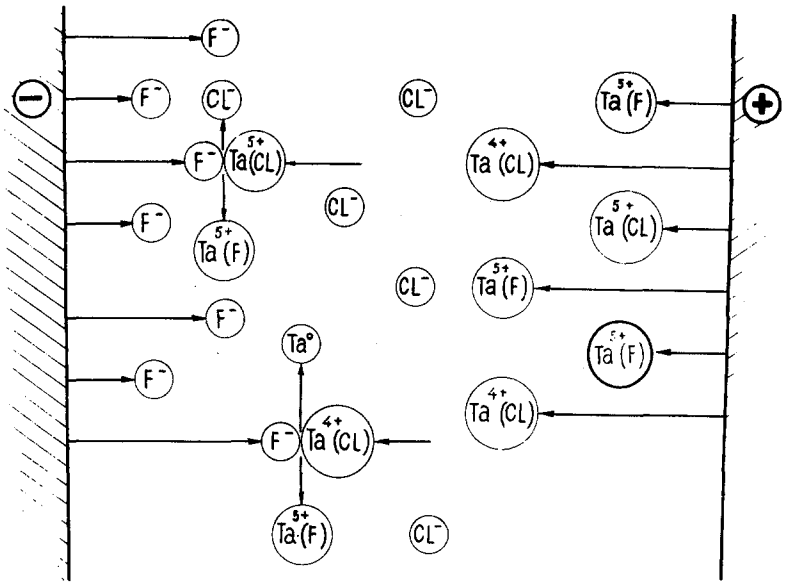

Fig. 11. Scheme of processes of Ta anodic dissolution and cathodic deposition in the CsCl–KCl–NaCl–K_2TaF_7 melt.

shell occurs. However when fluoride ions contact $Ta(IV)_{(Cl)}$ ions, a disproportionation Reaction 2 takes place with the formation of a suspension of metallic tantalum. The suspension contributes both to the sludge and the formation of the metal film growing out from the electrodes on the surface of the electrolyte. Convective fluxes are known to be intensified near the electrodes due to local temperature gradients. These electrolyte flows, enhanced with fluoride ions on the one hand and $Ta(IV)_{(Cl)}$ containing electrolyte on the other meet to produce typical films around the cathode at the gas/liquid boundary. The introduction of sufficient excess amounts of fluoride ions to the electrolyte [49] precludes the undesired side reactions.

4. Conclusions

The anodic dissolution of tantalum in NaCl–KCl–CsCl–K_2TaF_7 melts results in the formation of different oxidation states of tantalum, complexed to form different solution species designated $Ta(IV)_{(Cl)}$, $Ta(V)_{(Cl)}$, $Ta(V)_{(F)}$, whose relative amounts depend upon the K_2TaF_7 composition. This chemistry leads to an explanation of the formation of sludge and surface films which involves the fluoride ion driven disproportionation reaction involving $Ta(IV)_{(Cl)}$ complexes.

Acknowledgements

The authors gratefully acknowledge the assistance of Dr S. H. White, Wrentham, MA (USA), in the preparation of the text of this paper and his valuable criticism. The authors are also grateful to Prof. L. L. Lazutin for his help in preparation of the paper.

References

[1] A. N. Baraboshkin, 'Electrocrystallization of Metals from Molten Salts', Nauka (1976).
[2] D. Inman and S. H. White, *J. Appl. Electrochem.* **8** (1978) 375.
[3] J. Robinson, *in* 'Electrochemistry', vol. 8 (Specialist Periodical Reports), Sr. Rep. D. Pletcher, R.S.C., London (1983) p. 54.
[4] V. E. Komarov, M. V. Smirnov and A. N. Baraboshkin, *Trans. UFAN.* **3** (1962) 25.
[5] L. E. Ivanovskii, V. A. Lebedev, and V. N. Nekrasov, 'Anodic Processes in Halide Melts', Nauka (1983).
[6] S. A. Kuznetsov, A. L. Glagolevskaya, E. G. Polyakov and P. T. Stangrit, *in* 'High-Temperature Physical Chemistry and Electrochemistry', Sverdlovsk (1985) Ch. 1, p. 195
[7] I. F. Nichkov, S. P. Raspopin and V. I. Golubev, *Izv. Vuzov.* **4** (1962) 132.
[8] L. E. Ivanovskii and V. N. Diev, *Trans. UFAN.* **7** (1965) 73.
[9] *Idem, ibid.* **15** (1970) 36.
[10] Idem, *in* 'Physical Chemistry and Electrochemistry of Molten salts', Cimia (1968) p. 341.
[11] T. Suzuki, *Electrochim. Acta.* **15** (1970) 127.
[12] *Idem, ibid.* **15** (1970) 303.
[13] R. A. Bailey, E. N. Balko and A. A. Nobile, *J. Inorg. Nucl. Chem.* **37** (1975) 971.
[14] I. Nakagawa, *Nagoya Kogyo Gijutsu Shikeusho Hokoky* **23** (1974) 271.
[15] *Idem, Nippon Kagaku Kaishi.* **2** (1975) 255.
[16] S. H. White, D. Inman, R. Hug, T. Mukherjee and G. Warren, Ext. Abstr. 27th ISE Meeting, Zürich (1976) N254.
[17] G. F. Warren, S. H. White, D. Inman, *in* Proceedings of the 1st International Symposium on Molten Salts, Electrochemical Society (1975) 218.
[18] L. E. Ivanovskii and V. N. Diev, *Zash. Met.* **7** (1971) 499.
[19] A. N. Baimakov, A. M. Ezrohina and O. A. Sashinina, *Izv. Vuzov.* **1** (1985) 43.
[20] A. N. Baimakov and O. A. Sashinina, *Zh. Prikl. Chim.* **59** (1986) 439.
[21] P. Drossbach and P. Petrick, *Z. Electrochem.* **61** (1957) 410.
[22] I. D. Efros and M F. Lantratov, *in* 'Physical Chemistry of Molten Salts', Metallurgia (1965) p. 284.
[23] J. J. Rameau, *Rev. Int. Hautes Temp. Refract.* **8** (1971) 59.
[24] V. I. Konstantinov, E. G. Polyakov and P. T. Stangrit, *Electrochim. Acta.* **23** (1978) 713.
[25] A. N. Baimakov, S. A. Kuznetsov and P. T. Stangrit, *Electrochimia (Sov.)* **21** (1985) 597.
[26] S. Senderoff, G. W. Mellors and W. I. Reinhardt, *J. Electrochem. Soc.* **112** (1965) 840.
[27] D. Inman, R. P. Sethi and R. Spencer, *J. Electroanal. Chem.* **29** (1971) 137.
[28] P. Taxil and J. Mahenc, *Corr. Sci.* **21** (1981) 31.
[29] P. Taxil, *J. Less-Common Met.* **113** (1985) 89.
[30] P. Taxil and J. Mahenc. *J. Appl. Electrochem.* **17** (1987) 261.
[31] J. Hinden, I. Augustynski and R. Monnier, *Electrochim. Acta* **21** (1976) 459.
[32] S. Senderoff, *in* 'Modern Electroplating' (edited by F. A. Lowenheim), Wiley, New York (1974), p. 473.

[33] P. T. Stangrit, S. A. Kuznetsov, L. P. Polyakova and E. G. Polyakov, *in* Ext. Abstr. 6th Conf. Electrochim Nauka (1982) p. 282.
[34] S. H. White, *in* 'Molten Salts Techniques', Vol. 1 (edited by D. G. Lovering and R. J. Gale), Plenum Press (1983) p. 19.
[35] N. I. Puzinina, B. H. Kuliuzhin and V. G. Kamburg, *Zh. Phys. Chim.* **56** (1982) 2205.
[36] H. Shäfer and F. Kahlenberg, *Z. Anorg. Allgem. Chem.* **305** (1960) 178; **305** (1960); **331** (1964) 154.
[37] P. Pint and S. N. Flengas, *Trans. IMM* **87** (1978) 29.
[38] A. L. Glagolevskaya, S. A. Kuznetsov, E. G. Polyakov and P. T. Stangrit, *Zh. Prikl. Chim.* **61** (1988) 1036.
[39] S. A. Kuznetsov, E. G. Polyakov and P. T. Stangrit, *Izv. Vuzov* **4** (1982) 76.
[40] J. Painot, J. Hinden, J. Augustynski and R. Monnier, *J. Silicates Industries* **42** (1977) 57.
[41] Chen Guang-Sen, M. Okido and T. Oki, *J. Appl. Electrochem.* **18** (1988) 80.
[42] A. F. Alabyshev, M. F. Lantratov and A. G. Morachevskii, 'Reference Electrodes for Molten Salts', Metallurgia (1965).
[43] M. V. Smirnov, 'Electrodic Potentials in Molten Chlorides', Nauka (1973).
[44] L. P. Polyakova, B. I. Kosilo and E. G. Polyakov, *Electrochimia (Sov.)* **24** (1988) 892.
[45] I. S. Morozov and A T. Simonich, *Zh. Neorgan. Chem.* **11** (1957) 1907.
[46] H. Matsuda and G. Ayabe. *Z. Electrochem.* **59** (1955) 494.
[47] V. V. Safonov, B. G. Korshunov and Z. N. Shvetsova, *Zh. Neorgan Chim.* **9** (1964) 1409.
[48] Z. Galus, 'Theoretical foundations of electrochemical analysis', Mir (1974) p. 552.
[49] L. P. Polyakova, B. I. Kosilo and E. G. Polyakov, *Rasplavy* **2** (1988) 83.
[50] V. N. Kondratjev, 'Bond Rupture Energies', Nauka (1974).